Civil Engineering and Applied Solutions

Research Article

CEAS
Civil Engineering and Applied Solutions

Experimental and Numerical Investigation of Landfill Leachate Emission in Unsaturated Sandy Soils

Narges Soleimanian [a], Ali Akhtarpour [a*] , Mohammad Saleh Baradaran [a]

[a] Department of Civil Engineering, Faculty of Engineering, Ferdowsi University of Mashhad, Iran

ARTICLE INFO

ABSTRACT

This research represents a novel investigation into the infiltration of municipal waste landfill leachate into unsaturated sandy soil, with a particular focus on the propagation of pollutants. The significance of understanding pollutant emission in unsaturated soil is importance due to its profound environmental impact on ecosystems and its potential challenges to infrastructure development. The study examines key parameters, emphasizing initial matric suction and permeability, using both numerical and laboratory modeling techniques to compare pollutant emission under various conditions, including unsaturated soil in drying path and initially dry soil. Results reveal soil properties (density, permeability, water content) profoundly influence pollutant penetration. Advanced image processing estimates pollutant concentrations at different depths, offering accurate insights. The results derived from the image analysis were then compared with the outcomes obtained from the numerical modeling. This innovative approach holds promise for future applications and environmental monitoring. Findings aid strategies to mitigate landfill leachate effects, informing pollutant containment and prevention in unsaturated soil for sustainable environmental management.

1. Introduction

As urbanization accelerates, the growing prevalence of impermeable surfaces in infrastructures has sparked significant concerns regarding environmental sustainability [1]. These surfaces, which hinder water from naturally permeating into the soil, create an environment where pollutants and chemicals accumulated on the surface can easily infiltrate groundwater reserves. This disruption of natural water flow not only threatens the quality of underground water but also endangers aquatic ecosystems and poses risks to public health . The pollution of both groundwater and soil by contaminants, such as petroleum products and waste leachate, has emerged as a critical environmental challenge worldwide [2].

In this context, it becomes crucial to emphasize the importance of sustainability in all aspects of infrastructure development [3-5], especially in the construction of roads [6], soil stabilization [7], and concrete structures. By integrating sustainable practices into the design and construction of roads and infrastructures [8, 9], we can promote the natural infiltration of water, reduce environmental degradation, and improve the long-term resilience of urban spaces [10, 11]. Sustainable construction techniques, such as permeable pavements, eco-friendly soil treatment methods, and the use of environmentally responsible materials, are vital in mitigating the negative impact of urban development on the environment [12-14].

Incorporating these sustainable practices into the broader framework of urban planning and infrastructure development will ensure that infrastructures not only support economic growth but also protect natural resources, promote ecological balance, and improve the quality of life for urban populations [15, 16].

Pollution of underground water resources and soils by pollutants like petroleum products and waste leachate has become a major

---

How to cite this article: Soleimanian, N., Akhtarpour, A., Baradaran, M. S. Experimental and Numerical Investigation of Landfill Leachate Emission in Unsaturated Sandy Soils. Civil Engineering and Applied Solutions. 2026; 2(1): 58–73. doi:10.22080/ceas.2025.29684.1028.

global environmental issue. Soil contamination not only affects underground water tables but also impacts environmental geotechnics. Physical-chemical interactions between soil and pollutants can alter soil resistance, permeability, and compressibility, causing further problems. As pollutants move through unsaturated soil to groundwater, studies must consider unsaturated conditions. Investigating pollutant diffusion in subsurface soils and groundwater is crucial due to their potential widespread entry [17]. Effective rehabilitation of contaminated sites requires understanding pollutant behavior and propagation in subsurface layers. Identifying pollutant emission ranges is the first step in mitigating environmental damage [18, 19]. Knowledge of pollutant movement and accumulation is vital, considering the non-linear nature of fluid transfer in porous, heterogeneous environments [20]. Due to the complexity of factors involved, simple analytical solutions are not feasible at an executive scale.

Eltarabily and Negm [21] studied nitrate movement in different soils, including sandy ones, and evaluated vertical barriers for controlling contamination using FEM model. They found that soil properties significantly affect contaminant movement. They determined the best location and depth for installing sheet pile barriers to minimize contamination reaching groundwater. Szymański et al. [22] stated that closed municipal and industrial waste landfill sites can pollute groundwater. A landfill substratum can filter out pollutants. They research tests with a sand bed showed that filtration efficiency depends on pollutant mass, leachate intensity, and layer thickness. This method helps estimate safe filtration layer thickness. Sharma et al. [23] study quantifies leachate pollution and its effects on groundwater near four nonengineered dump sites in India. It assesses leachate and groundwater using the leachate pollution index (LPI), water quality index (WQI), and heavy metal pollution index (HPI). Results show high pollution levels, with water quality improving downstream. Principal component analysis (PCA) and hierarchical cluster analysis (HCA) identify pollution sources and zones. Javahershenas et al. [24] study assessed surface and groundwater pollution in Lahijan, over 9 months by landfill leachate. Parameters measured included temperature, turbidity, pH, COD, BOD5, metals, and ions. Results indicated elevated levels in the seasonal river, impacting water quality adversely according to the Water Quality Index.

Alghamdi et al. [25] assessed environmental risks associated with leachate from a landfill in Saudi Arabia. They analyzed leachate, groundwater, and soil samples for toxic elements, pH, EC, NO^{3-}, and E. coli. Results showed high concentrations of Fe, Mn, and Zn in leachate, unfit water for irrigation and drinking due to elevated metals and NO^{3-}, and significant soil contamination. The findings underscore the need for improved landfill management to mitigate environmental impacts. Hussein et al. [26] analyzed heavy metal contamination in leachate and surface soils from Malaysian landfills, highlighting significant threats to human health and the environment. Elevated As and Cr levels in leachate indicate progressive contamination. Non-sanitary, unlined landfills show higher metal concentrations compared to background levels. Indexes like Igeo, PI, and IPI confirm moderate to strong pollution in these areas, emphasizing the need for better landfill management to mitigate environmental impacts. Nyika et al. [27] investigates landfill leachate in South Africa, highlighting its potential to pollute groundwater due to high levels of conductivity, dissolved solids, and various ions exceeding WHO and SANS standards for drinking water. The leachate's pH of 4.7 renders it unsuitable for domestic use. Groundwater samples from different boreholes indicated contamination with metals and ions, attributed to decomposed waste infiltrating the resource. Recommendations include regular groundwater monitoring due to slow and unpredictable leachate movement. Alao [28] examines dumpsite leachate effects on soil and groundwater using geophysical and chemical analyses. Findings reveal widespread contamination, emphasizing urgent monitoring and remediation needs to protect groundwater. Depths below 23 meters are identified as potential sources of clean water amid compromised aquifers. Zango et al. [29] investigates the impact of enzymatic induced calcium carbonate precipitation (EICP), or biocementation, on fine-grained soil's hydraulic conductivity using digital image techniques (DIT). Results indicate EICP significantly alters leachate penetration patterns and reduces hydraulic conductivity. By the end of 28 days, treated soils saw reductions of 28.83% and 41.33% in hydraulic conductivity compared to untreated soil.

This research includes three laboratory parts, numerical modeling and image processing (Fig. 1). In the laboratory section, the distribution of municipal waste leachate in samples with different densities in two unsaturated and dry states has been investigated. In the numerical modeling section, SEEP/W and CTRAN/W packages from Geostudio software have been used to validate the samples made in the laboratory. In this way, the effect of the parameters affecting the transfer of pollutants in the soil environment such as the change in the underground water level, the relative density of the pollutant and the change in the dispersion coefficients have been investigated. In the third part, the image processing method was used to estimate the concentration of pollution in the soil so that by knowing the type of soil in real conditions, the concentration and diffusion process of the pollutant in the porous environment of the soil can be estimated relatively accurately and the results was compared with numerical modeling. It should be noted that the innovation of the present research is in 2 parts, investigating diffusion in unsaturated soil and using the image processing method in different concentrations.

2. Materials

2.1. Soil properties

In the current research, in order to test and investigate the effects of leachate contamination in the soil, the standard Firoozkooh No.131 sand has been used. Table 1 shows the geotechnical and chemical characteristics of this soil. Also, grain size distributions of this sand are given in Fig. 2.
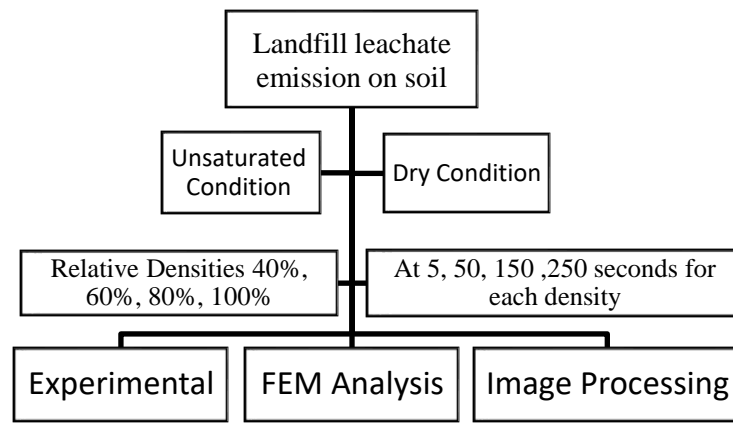
Fig. 1. Flowchart of research process.

Table 1. Geotechnical-chemical characteristics of firoozkooh No.131 sand [30, 31].

Geotechnical specifications	e_{max}	e_{min}	G_s	D_{50}	D_{10}	D_{60}
	1.091	0.710	2.656	0.65	0.45	0.67
Chemical characteristics (%)	SiO_2	Al_2O_3	Fe_2O_3	CaO	Na_2O	K_2O
	98.1	1.1	0.1	0.06	0.5	0.5
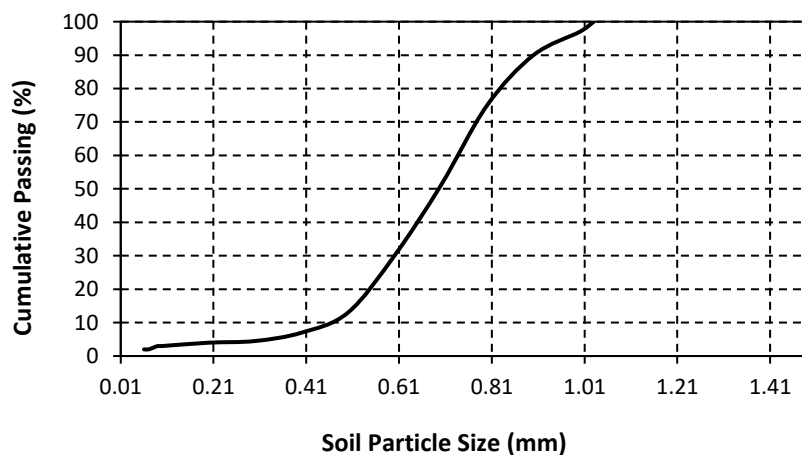
Fig. 2. Soil gradation curve of Firoozkooh No.131 sand.

2.2. Leachate characteristics

The leachate used in this research was prepared and combined with the specific weight of fat (cooking oils), protein (chicken rind), carbohydrates (bread), and fiber (vegetables and watermelon rind) in 11 days for each test to be more similar to municipal wastewater (Fig. 3). To ensure test repeatability, the combinations of leachate had to closely resemble one another. Each test required 4 liters of pollutant, which consisted of 3.5 liters of leachate, 100 cc of edible red colorant, and 400 cc of water. The addition of red colorant had aided in visually tracking the movement of the pollutant within the soil, allowing for straightforward observation and analysis. The characteristics of the leachate used in this research are shown in Table 2.

(a)

(b)

Fig. 3. (a) Produced rubbish after 11 days and (b) Collecting leachate for experimental procedure.

**Table 2. Characteristics of the leachate used in this research.**

Parameter	Unit	Value	Test Specification
pH	-	7.1	[32]
Ammonia	mg/L	2470	[33]
TSS	mg/L	14500	[34]
COD	mg/L	190100	[35]
BOD	mg/L	45500	[36]
TDS	mg/L	579	[37]

3. Method

3.1. Experimental investigation

This experiment was divided into two parts: the first part focused on unsaturated soil in the drying path, while the second part examined initially dry soil conditions. Each part of the experiment consisted of four tests, where the soil was subjected to different density levels: 40, 60, 80, and 100% in each test. To perform these tests, a rectangular glass cube measuring $120 \times 8 \times 80$ cm^3 with 1 cm thickness was specifically constructed as an experimental chamber to examine the movement of municipal landfill leachate through unsaturated soil. Fig. 4 shows the schematic view of the experimental setup and rainer system. The choice of a low thickness for the cube experimental box served two purposes: first, it allowed for a more detailed investigation of pollutant emission along the length and width of the soil, and second, it minimized two-dimensional numerical modeling errors. To ensure proper soil saturation and water table regulation, two valves were positioned at the bottom of the chamber (Fig. 4a). These valves were covered with geotextile material to prevent sand from being washed away during water entry and exit. To achieve uniform filling and reach the desired densities of the soil in the experimental box, a carefully designed rainer system was employed (Fig. 4b).

To perform the first part of the experimental test, the container box was filled with soil up to a height of 60 cm, and then the bottom valves were opened to ensure complete soil saturation with water. Following saturation, the container remained untouched for a 24-hour period to facilitate the release of any trapped air bubbles. Afterward, the water level was regulated by opening the lower valves, lowering it to around 10 cm from the container's bottom, considering the capillary level (Table 3). Then, a 24-hour period was provided for the soil to attain equilibrium relative humidity before introducing the pollutant for penetration.
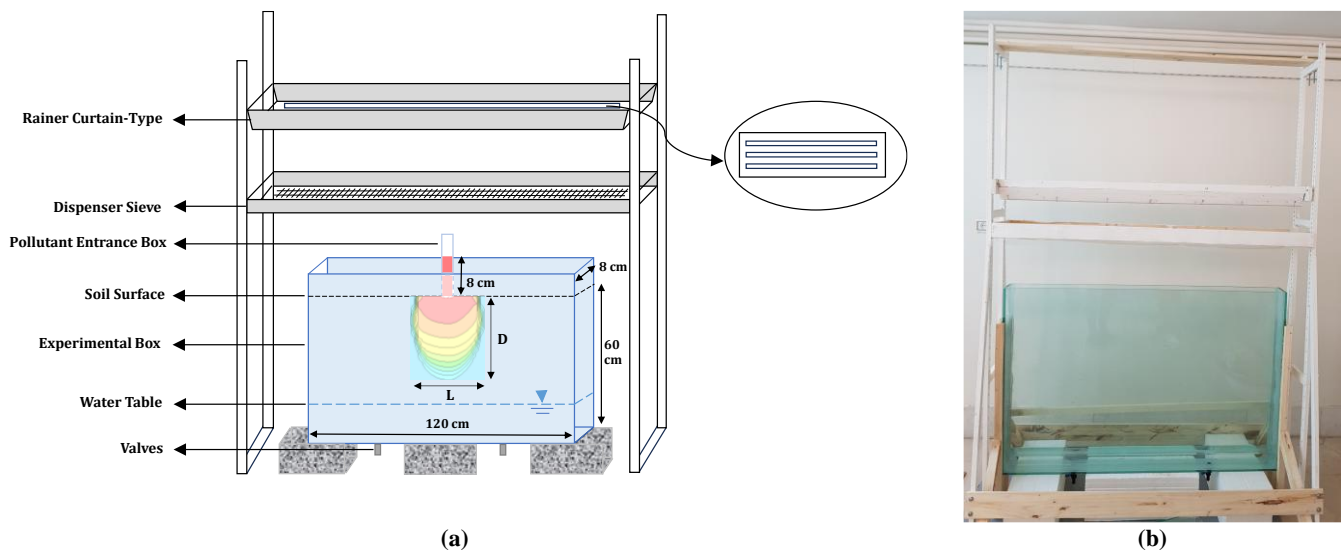
Fig. 4. (a) Schematic of experimental setup and (b) Chamber (container) box and rainer system.

Table 3. Mechanical specifications of the expanded masonry unit.

Density (%)	40	60	80	100
Capillarity level (cm)	6	7	8	8

To perform the second part of the experimental test, the container box was also filled with soil up to 60 cm, and the bottom valves were opened to allow water to reach the desired height of 10 cm, considering the capillary level (Table 3). The difference between the second part and the first part was that the soil was not saturated in the second part (Fig. 5). Then, similar to the first section, a 24-hour period was provided for the soil to attain equilibrium relative humidity. Afterward, the pollutant penetration process was initiated. As shown schematically in Fig. 4a, the pollutant penetrated into the soil through a rectangular glass cube chamber with dimensions of $20 \times 7 \times 3$ cm^3 and with a fixed head of 3 cm. The pollutant chamber is placed in the center of the glass box due to symmetry. In the second part, just before the pollutant penetration, soil sampling was conducted using a PVC tube with a diameter of 3 cm, enabling the collection of soil samples from different depths. The water content at various depths was then

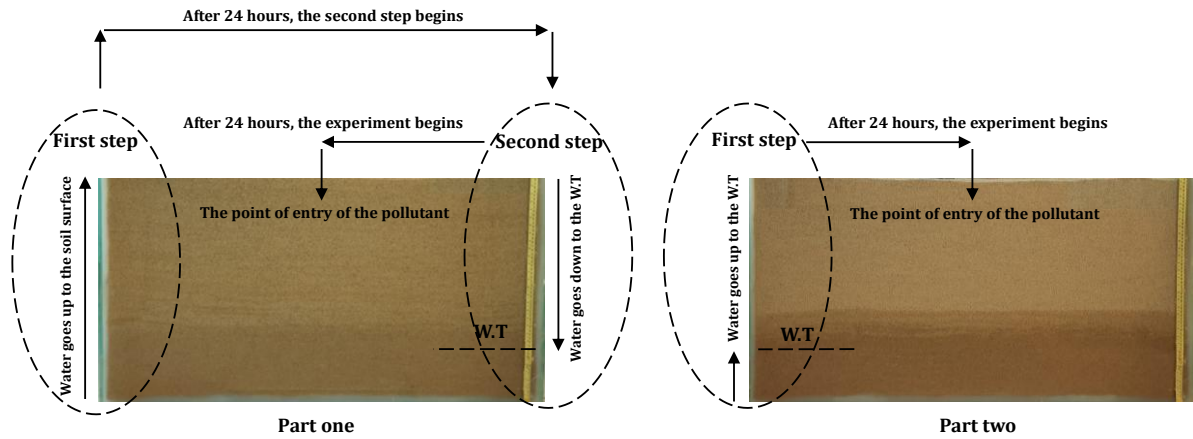measured to obtain a water content profile before the testing began (Fig. 6).

Fig. 5. The difference between part one (Unsaturated soil in drying path) and part two (Initially dry soil) of experimental tests.
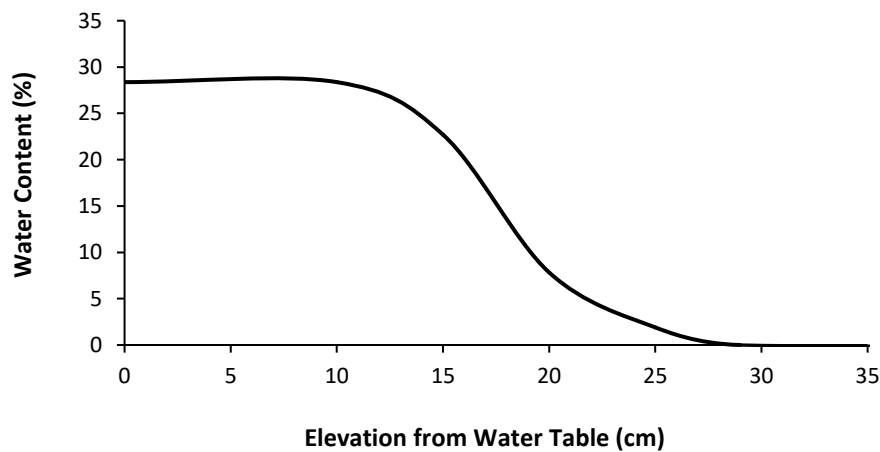

Fig. 6. Percentage of water content in the depth of the soil.

3.2. Numerical modeling

In this research, SEEP/W and CTRAN/W packages from Geostudio were used to model pollutant emissions. The Density-Dependent Analysis in SEEP/W, which combines CTRAN and SEEP, was utilized to study emissions under various relative densities. SEEP/W, developed by GeoStudio, specializes in modeling groundwater flow through porous media like soil [38, 39]. Understanding hydraulic conditions is crucial for investigating pollutant emissions in such media, as they directly affect contaminant transport. Appropriate material properties, such as soil hydraulic conductivity, were defined to represent these conditions and simulate pollutant transport. Defining the soil-water characteristic curve (SWCC) is very important to estimate the behavior of unsaturated soil. As input parameters for defining the SWCC curve, the saturated permeability (Table 4) and specifications of the 131 standard Firoozkoh sand were determined through experimental measurements (Table 1). Fig. 7 illustrates the functions of the SWCC curve for the unsaturated soil for 131 standard sands of Firoozkooh at different density.

Table 4. Firoozkooh sand soil properties in numerical modeling.

Density (%)	Saturated permeability (m/s)	Porosity
40	79×10-5	0.927
60	51×10-5	0.848
80	30×10-5	0.769
100	15×10-5	0.69

Through mesh studies, the mesh dimensions were set to 0.02 m2, and nine Gaussian points were used to ensure accurate representation. The boundary conditions of the model included specifying the groundwater table elevation (10 cm depth from the bottom of the model), using a constant head for the region of pollutant penetration, and using a spatial function for pressure head that was applied to establish varying pressure head values at different depths above the water table [40].
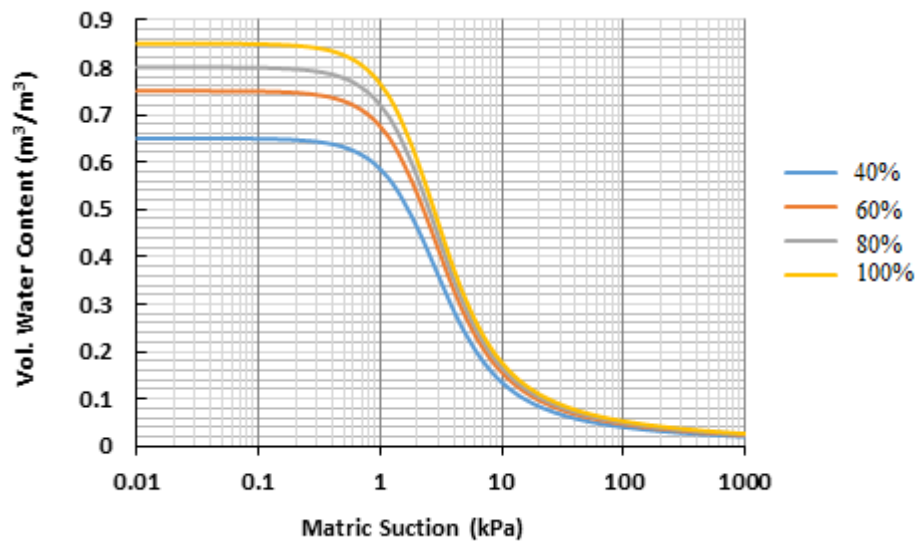
Fig. 7. SWCC curve for unsaturated soil in different densities.

In dry conditions, by utilizing available water content profiles at different depths and applying Eqs. 1 and 2, the volumetric water content can be calculated for each depth. Consequently, the water negative pressure head can be obtained by referring to the SWCC curve for each respective depth.

$$Sr.W = Gs.e \qquad (1)$$

$$Sr.n = \theta \qquad (2)$$

In these Equations, S_r, w, e, G_s, n, and θ, represent degree of saturation, water content, void ratio, specific volume, porosity, and volumetric water content respectively. Fig. 8 shows a difference in water negative pressure head between unsaturated soil in the drying path and initially dry soil.

| (a) | (b) |
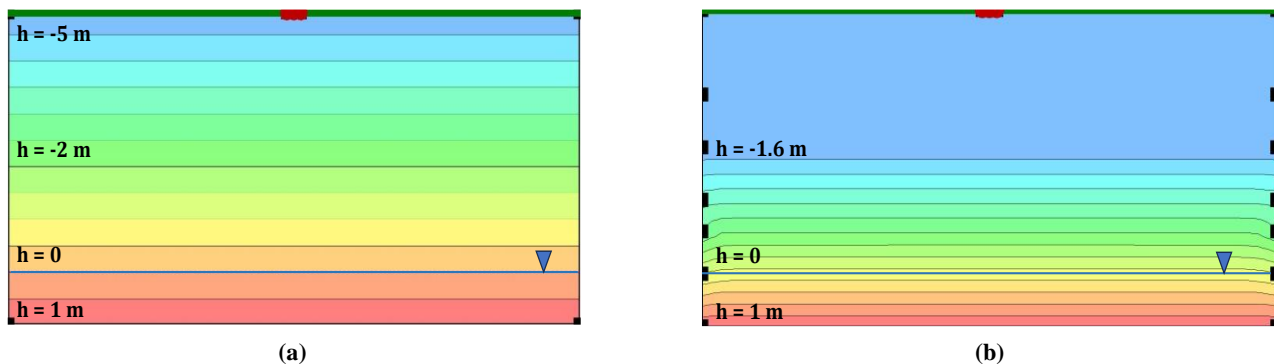
Fig. 8. Comparison water negative pressure head between (a) unsaturated soil in drying path and (b) initially dry soil.

The SEEP/W model was converted to CTRAN/W, requiring the determination of pollutant attributes like diffusion and dispersion. Using Kuo [41] guidelines, the diffusion coefficient and dispersion coefficients were set, longitudinal dispersion coefficient of 0.1 times the length of the relevant dimensions. Pollutant entry conditions were defined at a constant concentration of 1 g/m³, and the model was analyzed with specific time steps. Parameters used in SEEP/W and CTRAN/W are detailed in Table 5, with pollutant emission analyzed for dry and unsaturated soil at 5, 50, 150, and 250 seconds.

Table 5. Numerical model details.

Parameter	Unit	Value
The relative density of pollutant	-	1.2
Pollutant head	cm	3
The water level of groundwater	cm	10
Longitudinal Dispersivity	m	0.12
Transverse Dispersivity	m	0.06
Diffusion	m²/s	10-9
Time	s	400
Width of the model	cm	60
Length of model	cm	120

3.3. Image processing

In this study, MATLAB was used for image analysis. Images from an experimental chamber box containing soil and pollutant emissions were processed to generate visual representations in the form of curves. These curves illustrated changes in color intensity across pixels at varying soil depths, revealing pollutant distribution and behavior. Initially, a pre-leakage image was captured to document the test box and lighting conditions. Consistent lighting was maintained for subsequent images taken at various leakage stages. Images, originally in RGB color space, were converted to grayscale using a binary filter and then transformed into HSV color space, focusing on the value band. Average and median filters were applied to reduce noise. Figs. 9 and 10 illustrate the image processing algorithm with the applied filters.

(a)   **(b)**   **(c)**
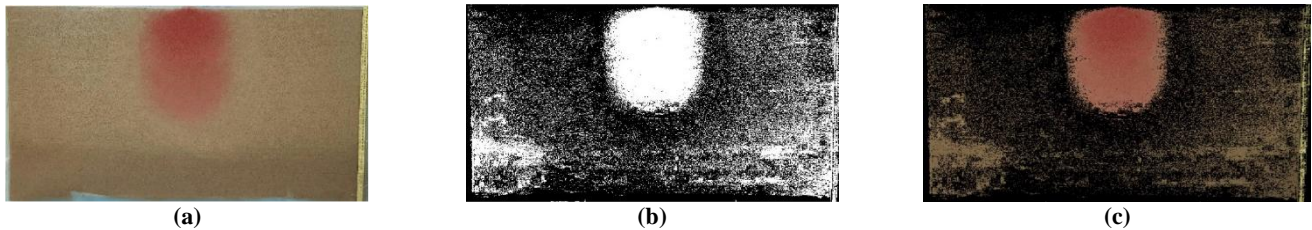
Fig. 9. Function of image processing algorithm (a) Image in RGB color space, (b) Image in binary space, (c) Using binary image as a filter on RGB image.

(a)   **(b)**   **(c)**
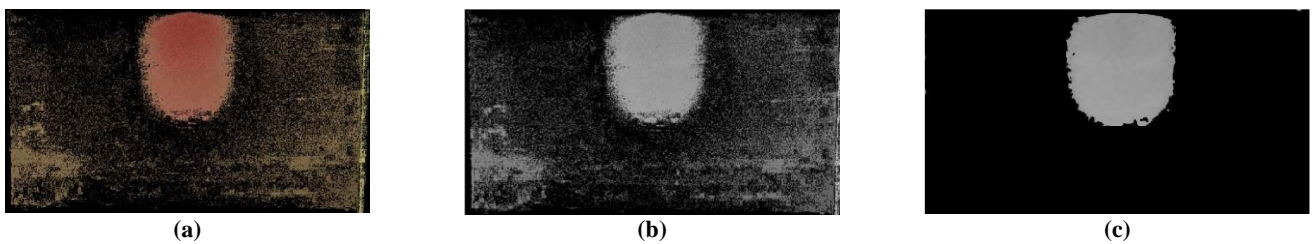
Fig. 10. Using average and median filter on image (a) Using binary image as a filter on RGB image, (b) Image in HSV color space, (c) Filtered image.

A curve showing color intensity variation with soil depth was plotted (Fig. 11a), then transformed into a concentration curve proportional to depth. The curves were calibrated to show 100% concentration at maximum color intensity and 0% at minimum. Due to inherent noise, a linear function fit was applied to compare these curves with concentration curves derived from the FEA. Fig. 11b shows the concentration change curve with respect to depth, as produced by GeoStudio.
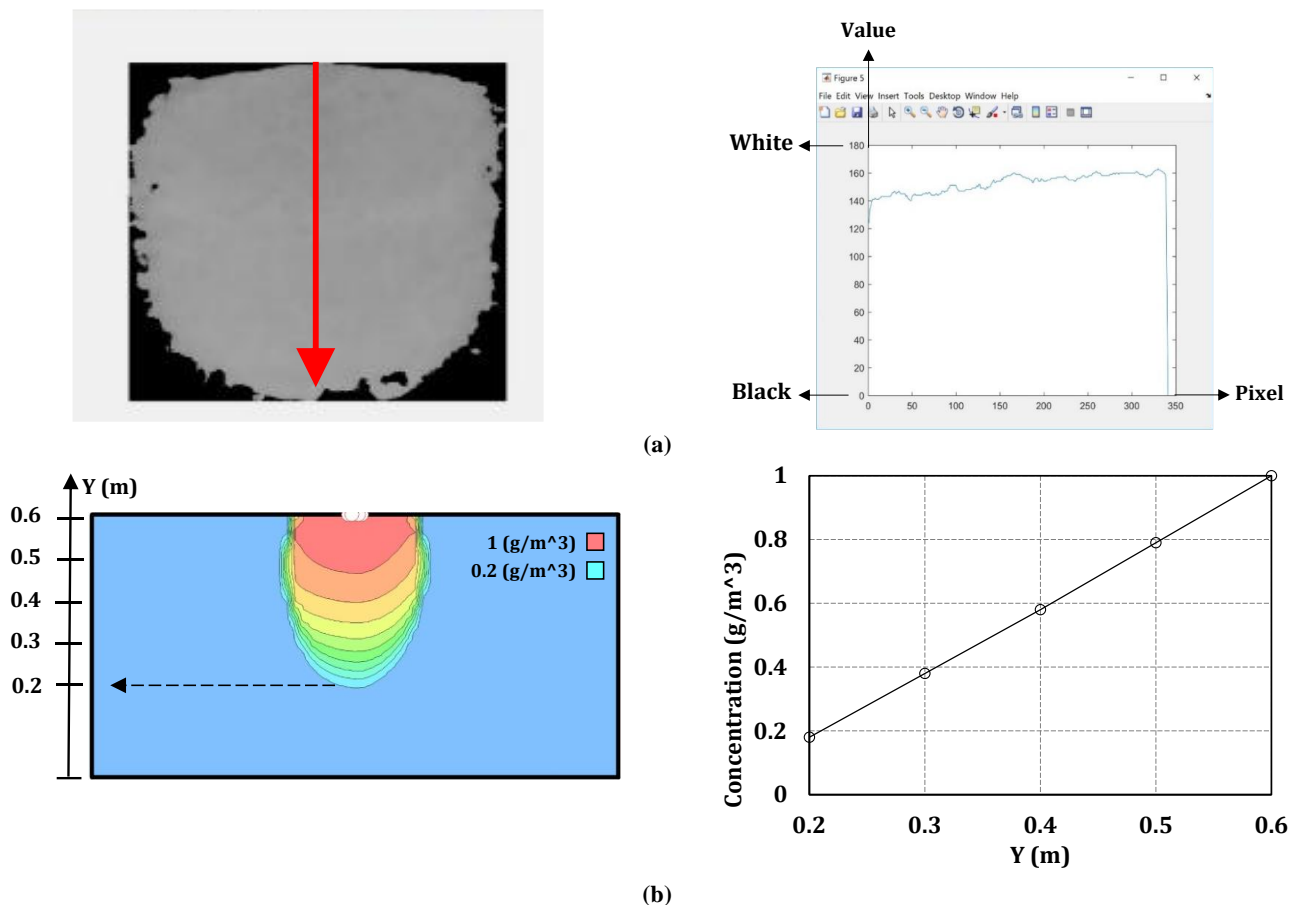

(a)

(b)

Fig. 11. Change in concentration in soil depth estimated by (a) MATLAB (b) Numerical analysis.

4. Results and discussion

4.1. Density and condition impact on penetration depth

Fig. 12 compares pollutant penetration in different soil densities under both dry and unsaturated conditions. The experimental results indicate that pollutants tend to penetrate dry soil at a faster rate compared to unsaturated soil. Capillary forces, caused by the surface tension of moisture in soil pores, play a crucial role in slowing down the movement of pollutants in unsaturated soil. When soil is unsaturated, these capillary forces tend to retain moisture within the soil matrix, making it more difficult for pollutants to infiltrate. In dry soil, these capillary forces are largely absent, allowing pollutants to move more freely through the larger air-filled pores. Moreover, Unsaturated soil typically contains some moisture that can interact with pollutants through sorption (absorption processes). These interactions can temporarily hold pollutants in the soil and reduce their mobility. In contrast, dry soil has limited or no moisture content to facilitate these sorption mechanisms, resulting in less resistance to pollutant movement. On the other hand, in unsaturated soil, the presence of water leads to higher viscosity, which creates more drag on pollutant particles as they move through the soil. In dry soil, with minimal moisture content, the viscosity is lower, resulting in reduced resistance to pollutant penetration.
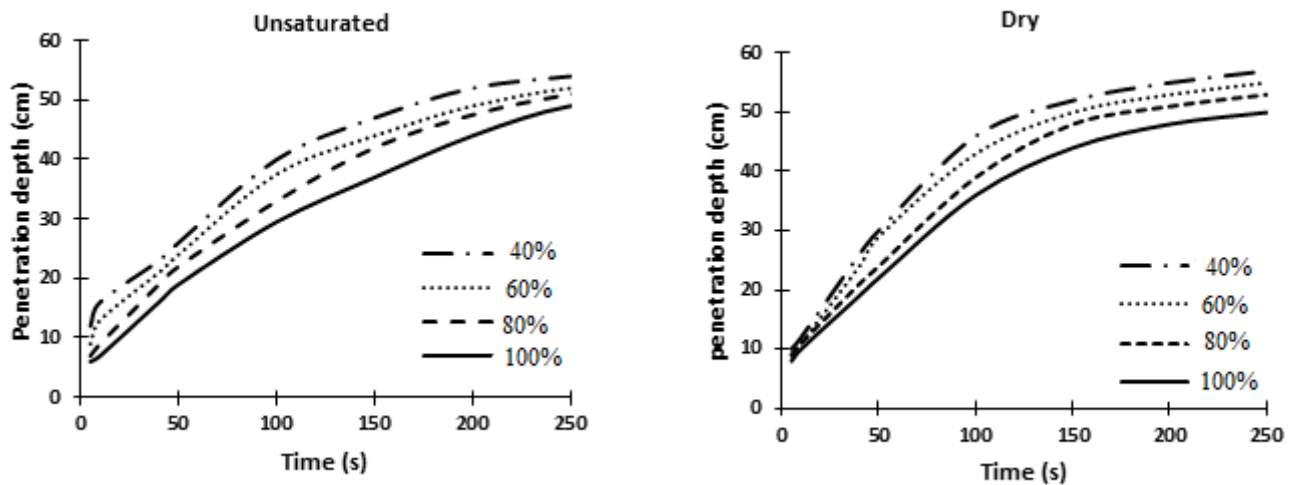

Fig. 12. Penetration depth of the pollutant by passing time in different densities in experimental tests on unsaturated and dry soil.

Fig.s 13 and 14 present a comprehensive comparison between numerical analysis and experimental test results for different densities. The curves depicted in Fig.s 13 and 14 demonstrate a satisfactory level of consistency between the numerical and experimental states. The results show that the numerical models estimate the pollutant penetration into the soil in unsaturated soil about 4% more than the experimental models. This is while the numerical models estimate the pollutant penetration into the soil in dry soil with 100% density about 5% less than the experimental models.
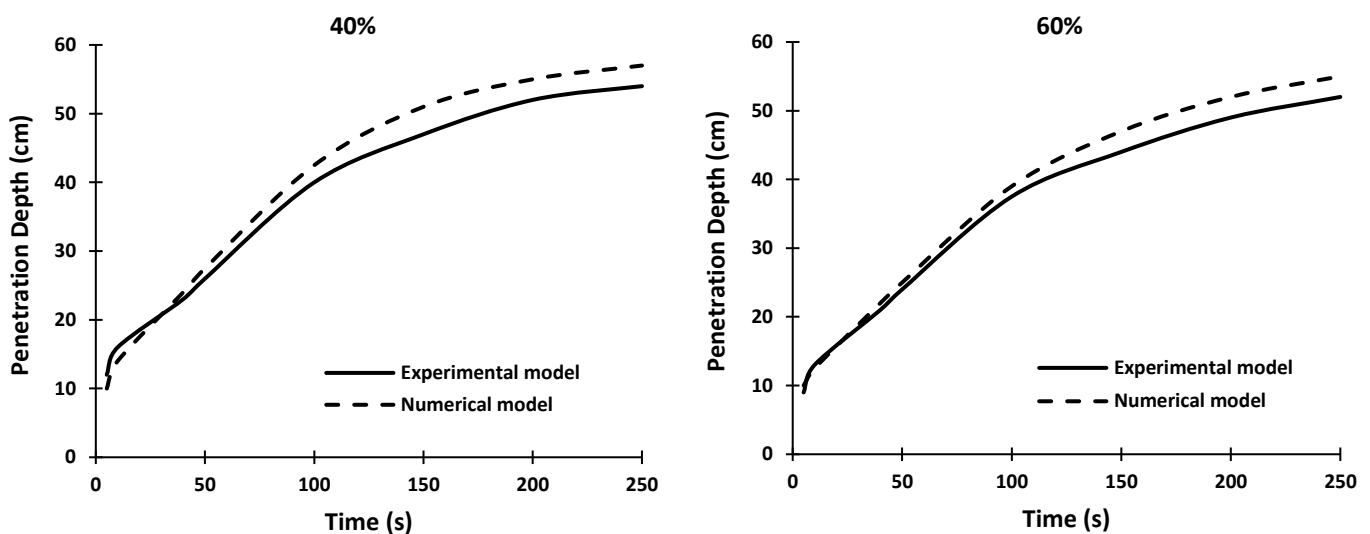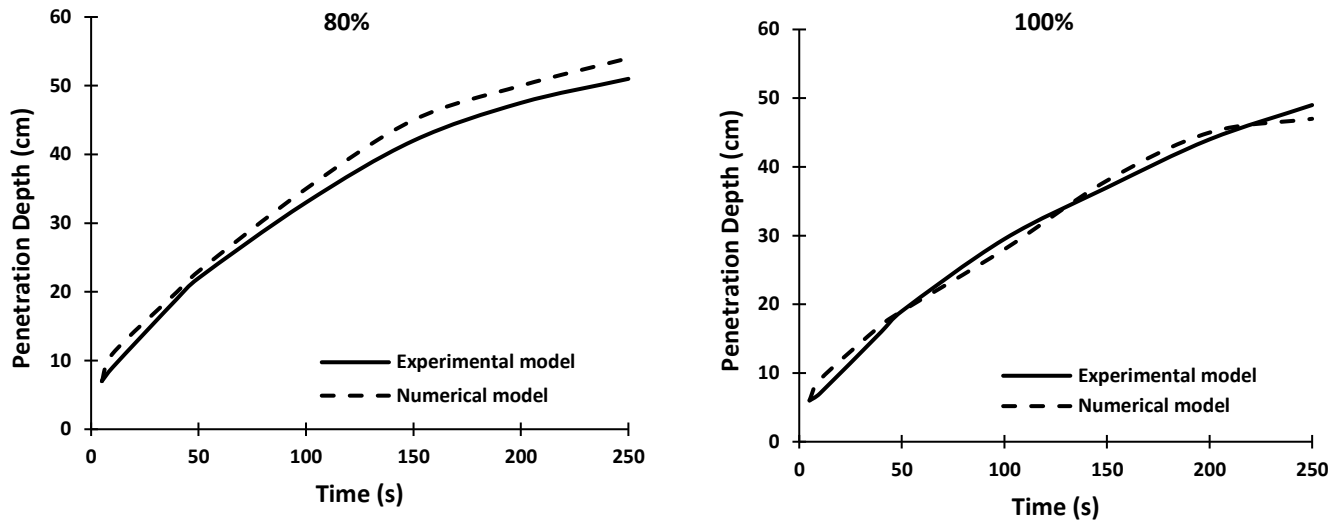
Fig. 13. Comparison between the results of numerical analysis and experimental test in unsaturated soil for different densities from 40% to 100%.
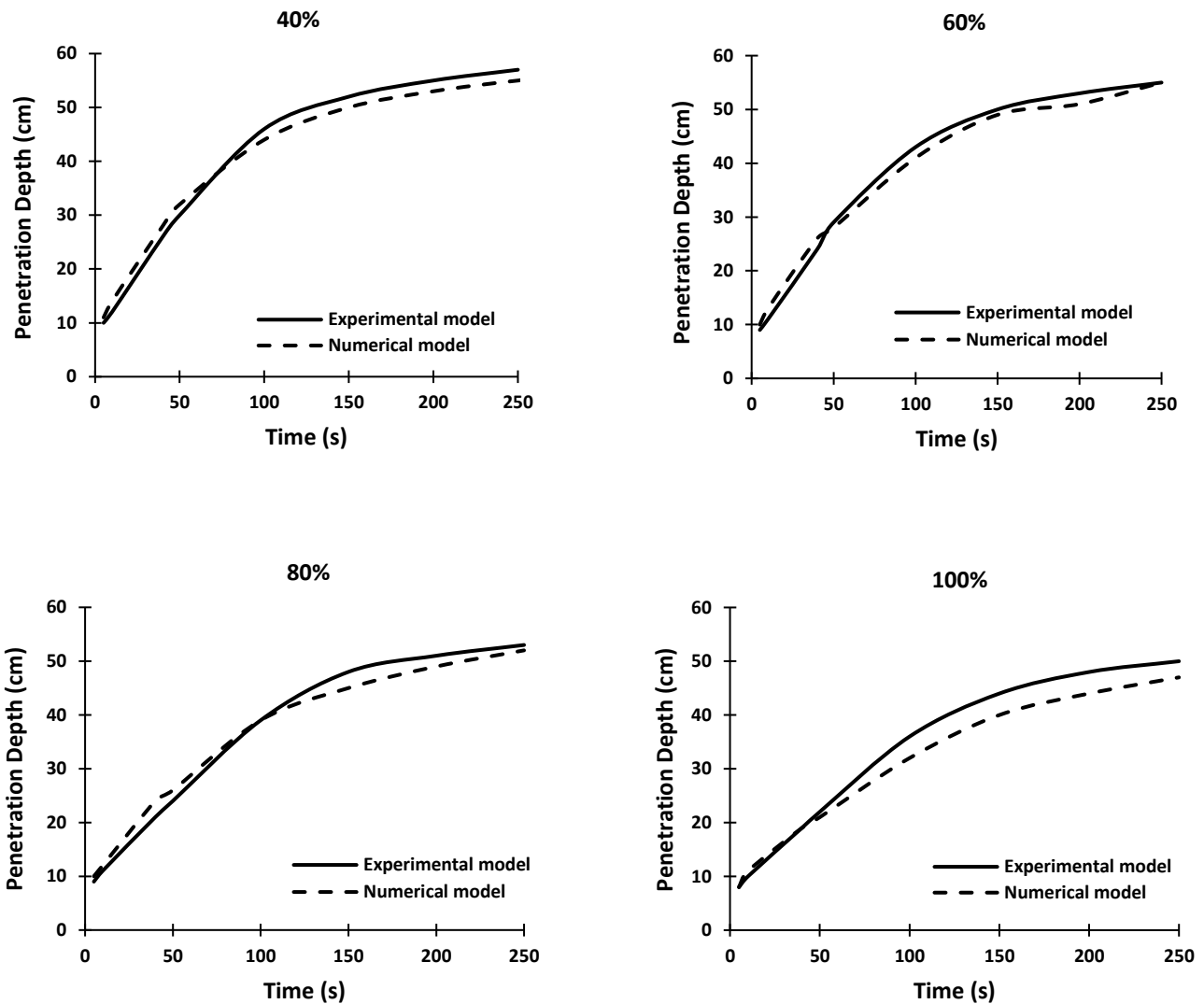
Fig. 14. Comparison of the results of numerical analysis and experimental test in dry soil for different densities from 40% to 100%.

4.2. Density and soil condition impact on penetration time

The time for the pollutant to reach the underground water (deep penetration) in four tests performed in unsaturated and dry conditions is presented in Fig. 15. As can be seen from the results, at the same density, the time of reaching the pollutant in dry soil is much less than that in unsaturated soil, which has been confirmed in previous researches. Also, according to the results of Fig. 15, it can be said that with the increase in the relative density of the soil, the time for the pollutant to reach the underground water has increased. The reason for this is that increasing the relative density of the soil reduces the empty space and porosity of the soil, reduces the hydraulic conductivity, and increases the resistance to the flow of water and pollutants. As a result, the speed of movement of pollutants decreases and the time they reach the underground water increases.
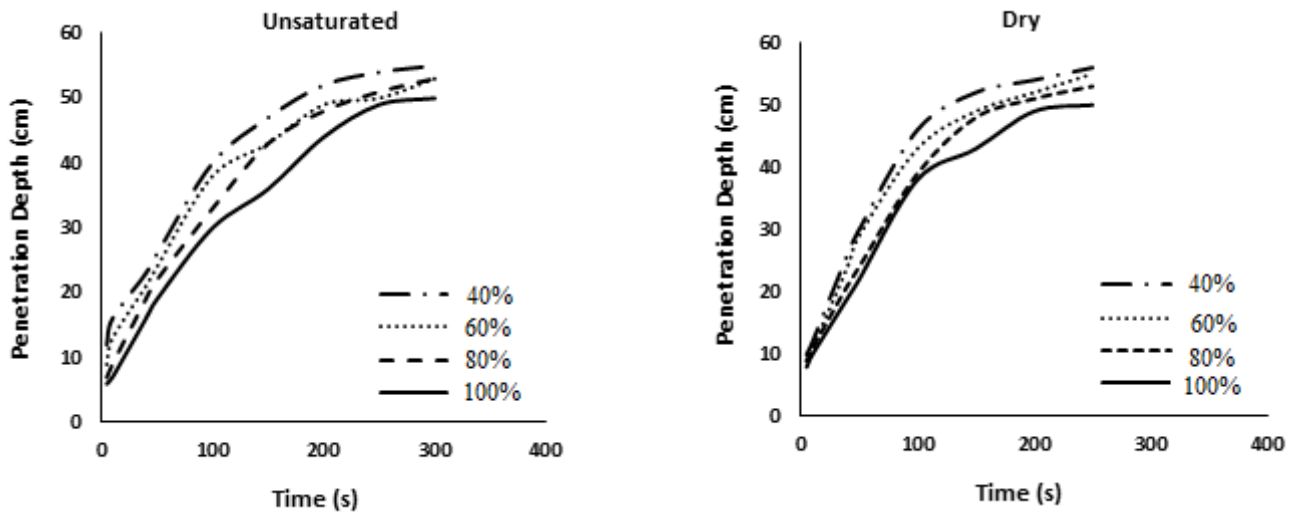
Fig. 15. Penetration time of pollutant at different densities on unsaturated and dry soil.

4.3. Longitude dispersivity

Based on the given explanation, it is expected that longitudinal dispersivity of pollutants in unsaturated soils is greater than that in dry soil (Fig. 16). According to the results of Fig. 16, longitudinal dispersivity in unsaturated soil is about 25 to 40% more than that in dry soil. This increase can be attributed to the presence of water in unsaturated soils, which enhances diffusion and advection processes. Water films around soil particles create pathways that facilitate pollutant movement, leading to higher dispersivity. Additionally, soil-water interactions affect hydraulic conductivity and porosity, promoting more extensive mixing and spreading of contaminants. Capillary forces in unsaturated soils also play a role by creating preferential flow paths, increasing overall dispersivity. These findings highlight the importance of considering soil moisture when evaluating pollutant dispersivity. The observed 25 to 40% increase in dispersivity in unsaturated soils emphasizes the need for detailed hydrogeological studies to accurately predict and manage pollutant spread in different soil conditions.
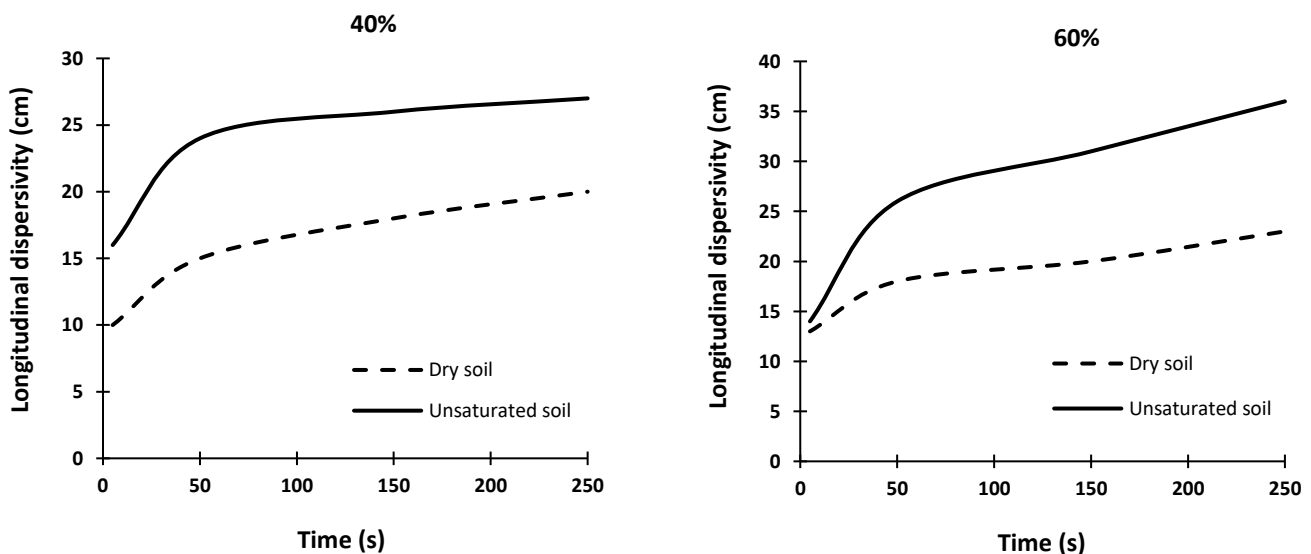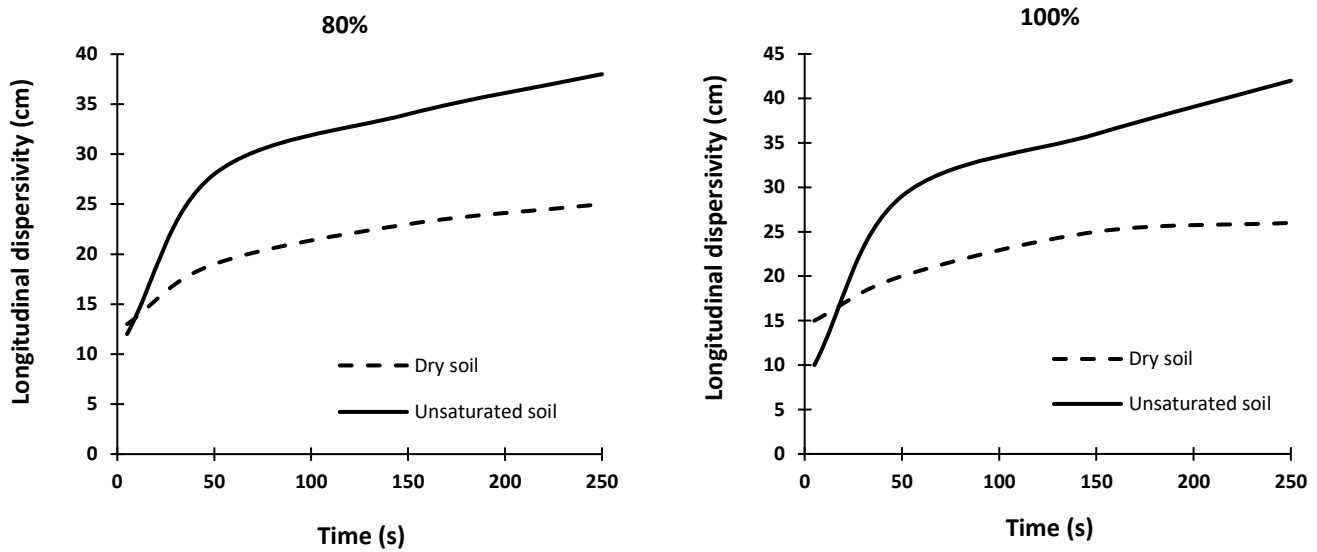
Fig. 16. Comparison of longitudinal dispersivity of pollutants in unsaturated and dry soil with different densities from 40% to 100% in experimental tests

Subsequently, Figs. 17 and 18 provide a comparison between pollution emissions in a numerical and an experimental model specifically at 100% density for unsaturated and dry condition, respectively. Based on the results, an intriguing phenomenon comes to light: in the dry soil, the penetration rate of pollutants into the soil depth is notably greater than their longitudinal expansion, a phenomenon that is not seen in unsaturated soil. Several factors contribute to this intriguing observation. Firstly, in dry soil, the absence of moisture limits lateral movement, causing pollutants to predominantly travel in the path of least resistance, vertically downward. Without the presence of water to aid in lateral dispersion, pollutants are more likely to percolate deeper into the soil, potentially reaching groundwater reservoirs and posing a heightened risk to water quality. Secondly, the compacted nature of dry soil hinders the spread of contaminants laterally, leading to a concentration of pollutants in the immediate vicinity of their source. Thus, the combination of limited horizontal movement and enhanced vertical penetration results in a higher potential for contaminants to infiltrate deeper soil layers, necessitating increased vigilance in managing pollutant sources and their potential long-term impacts on soil and water ecosystems.
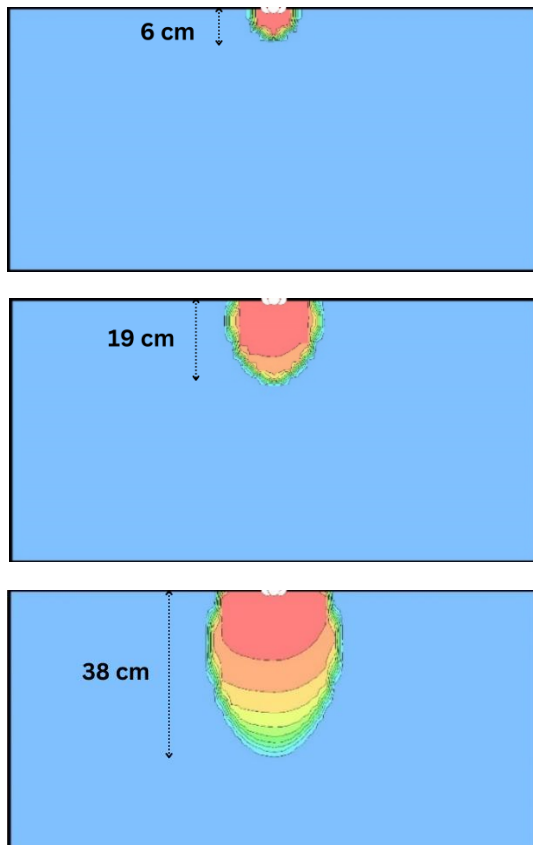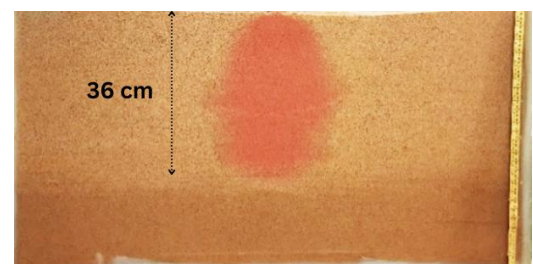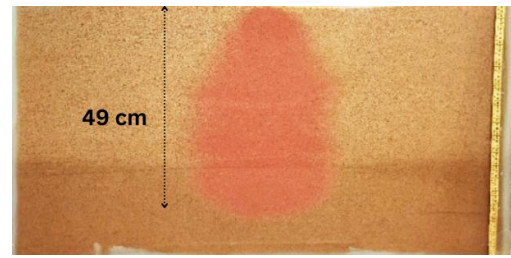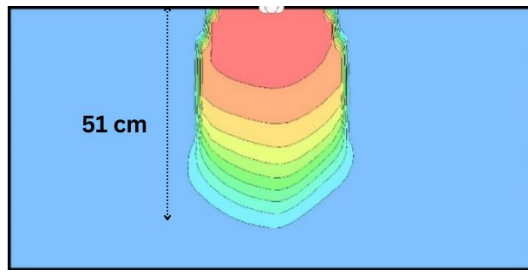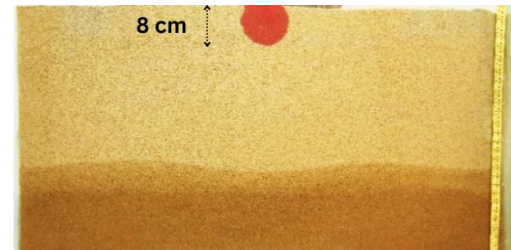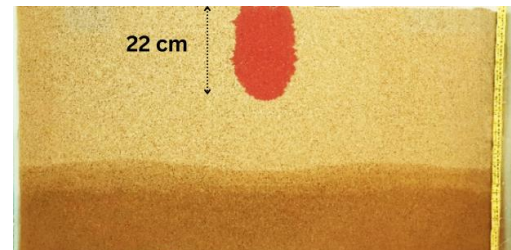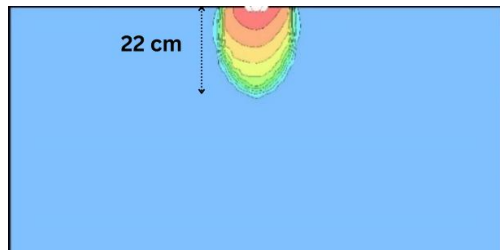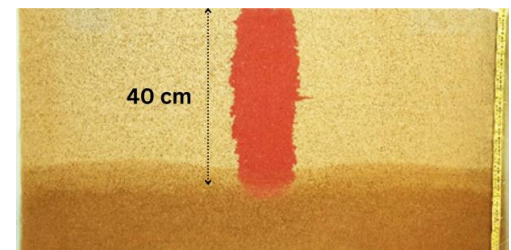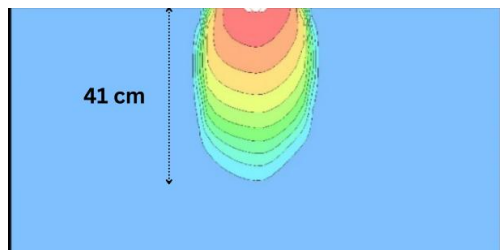

(a)
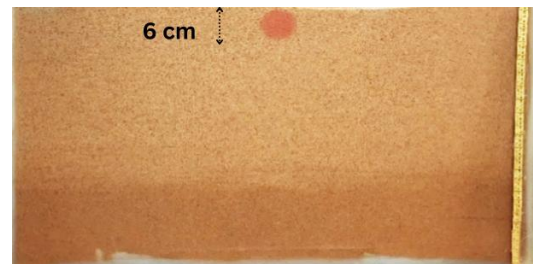
(b)
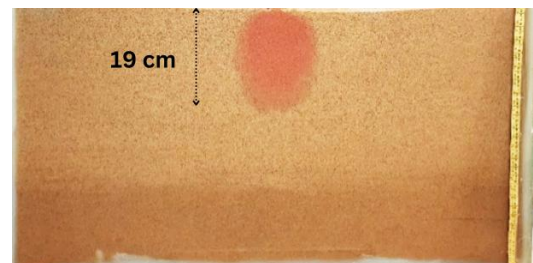
(c)

(d)

Fig. 17. Comparison between pollution emission in the experimental test and numerical analysis at unsaturated soil with 100% density at times: (a) 5, (b) 50, (c) 150, and (d) 250 second.
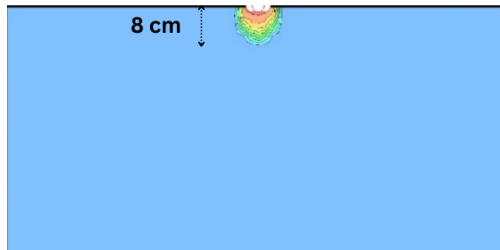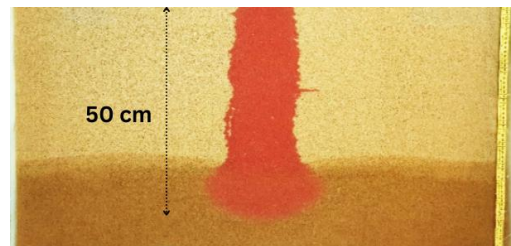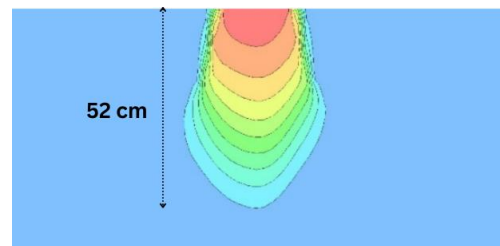

(a)

(b)

(c)

(d)

Fig. 18. Comparison of pollution emission in the experimental test and numerical analysis at dry soil with 100 % density at times: (a) 5, (b) 50, (c) 150, and (d) 250 second.

4.4. Verifying image processing analysis

In this analysis image analysis method was used for estimating the pollutant penetration in depth of sandy soils. For sandy soils with densities ranging from 40% to 100%, Fig. 19 shows a comparison of the curves generated from image analysis and finite elemental models (GeoStudio). Based on the depicted curves, it can be observed that the concentration curves obtained from both image analysis and FEM exhibit a similar rate of decline. As a result, it appears that these approaches can accurately (and with a small margin of error) predict the soil pollution concentration. Differences between image analysis and FEM curves reduced approximately from 8% to 1% as soil density increased. It should be noted, though, that the variation in backdrop color within the soil saturation region impacts the intensity of the pollutant's color when it enters the groundwater. Consequently, image analysis may not accurately predict the concentration in such cases. It is, therefore, recommended to focus on examining the concentration

changes near the boundary between the pollutant and the groundwater level, where the impact of color intensity variations is prominent.
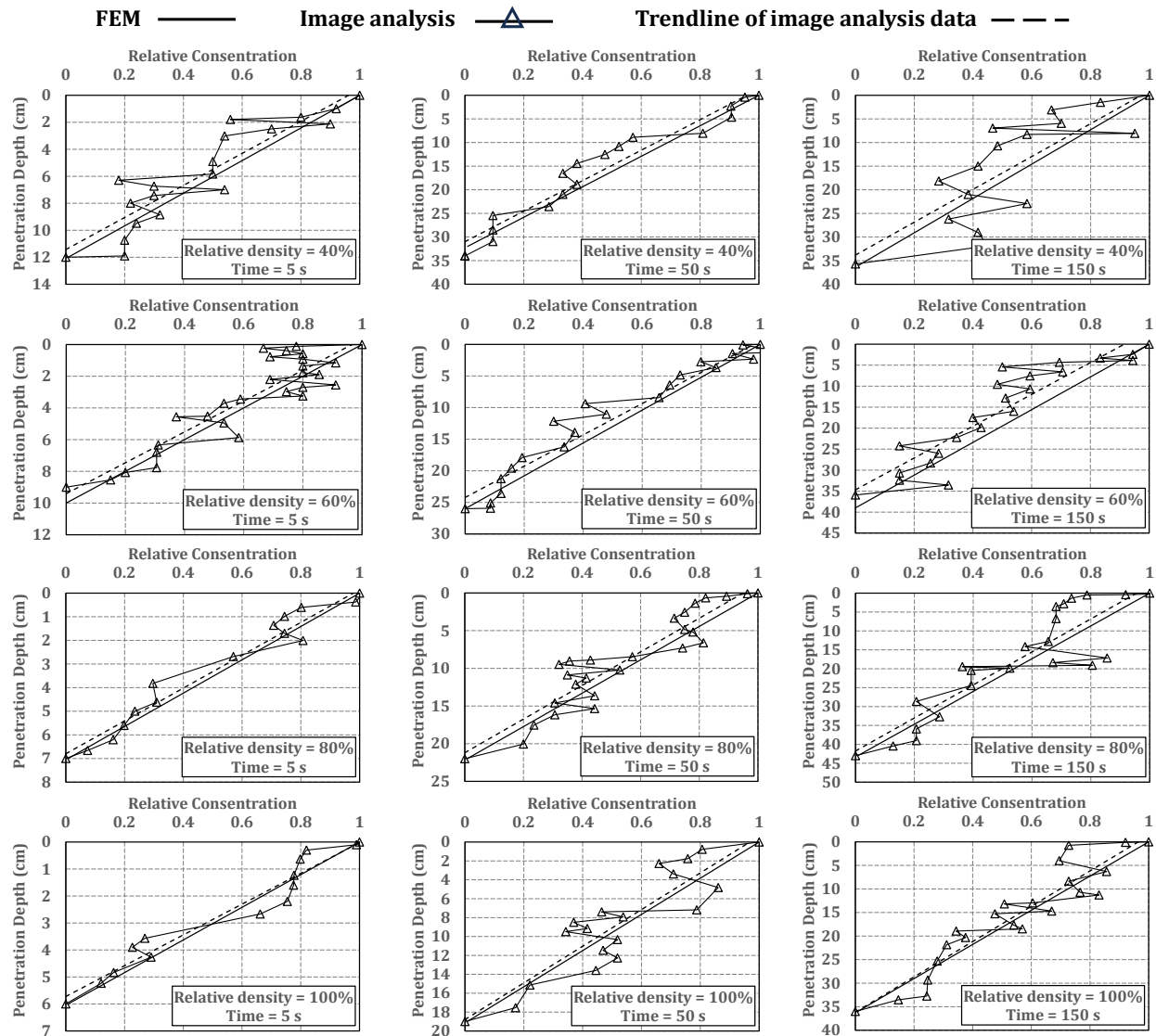
FEM ———   **Image analysis** —△—   **Trendline of image analysis data** — — —

Fig. 19 Comparison of concentration curve in FEM and image analysis in soil (to the level of groundwater).

5. Conclusions

In recent years, the pollution of underground water resources and soils by pollutants such as petroleum products and waste leachate has become a serious global environmental problem. Soil contamination affects underground water tables and impacts environmental geotechnics, as physical-chemical interactions between soil and pollutants can alter soil properties like resistance, permeability, and compressibility, leading to potential issues. Since soil is often in an unsaturated state when pollutants are released, studies and modeling must consider unsaturated conditions. This research aims to investigate the distribution of municipal waste leachate in unsaturated and dry soils, identify effective parameters in unsaturated soils, develop a numerical model to predict leachate release, and use image processing to estimate pollution concentration and compare it with the numerical and experimental models. The key findings are as follows:

- Discrepancies in longitudinal pollutant expansion between numerical and experimental models may result from slight errors in laboratory measurements and the anisotropic nature of permeability.

- Relative density, permeability, matric suction, gradient, and water content are key parameters influencing pollutant emission.

- Increasing relative density reduces pollutant penetration depth but increases longitudinal penetration.

- Pollutant penetration in initially dry soil is faster compared to unsaturated soil in the drying path due to increased gradient.

- Image processing accurately estimates pollutant concentration at different depths in soils even before reaching the water table.

- Numerical, experimental, and image processing results show good agreement with each other.

- Increasing soil density leads to improved consistency between image processing and finite element model results.

Statements & Declarations

References

[1] Ayar, P., Baradaran, S., Abdipour Vosta, S. A Review on the Effect of Various Additives on Mechanical Properties of Stone Mastic Asphalt (SMA). Road, 2022; 30: 57-86. doi:10.22034/road.2021.295635.1969.

[2] Almahmodi, R., Abdalhusein, M. M., Akhtarpour, A., Mahmood, M. S. Characterization of collapsible gypsum sand soil with the presence of matric suction using a modified odometer apparatus. The International Journal of Advanced Manufacturing Technology, 2022; doi:10.1007/s00170-022-10146-x.

[3] AlNaddaf, H. Q. A., Kouzegaran, S., Akhtarpour, A., Fattah, M. Y. Effects of Cement Treatment on the Behavior of Unsaturated Gypseous Soils. Transportation Infrastructure Geotechnology, 2025; 12: 140. doi:10.1007/s40515-025-00602-y.

[4] Baradaran, S., Aliha, M. R. M., Maleki, A., Underwood, B. S. Fracture properties of asphalt mixtures containing high content of reclaimed asphalt pavement (RAP) and eco-friendly PET additive at low temperature. Construction and Building Materials, 2024; 449: 138426. doi:10.1016/j.conbuildmat.2024.138426.

[5] Baradaran, S., Ameri, M. Investigation of Rutting Failure in Asphalt Mixtures and Its Improvement Strategies. Road, 2023; 31: 53-70. doi:10.22034/road.2022.337945.2041.

[6] Baradaran, S., Rahimi, J., Ameri, M., Maleki, A. Mechanical performance of asphalt mixture containing eco-friendly additive by recycling PET. Case Studies in Construction Materials, 2024; 20: e02740. doi:10.1016/j.cscm.2023.e02740.

[7] Balighi, M., Baradaran, M. S., Akhtarpour, A. Numerical investigation of swelling soil behavior and its effect on gas well casing internal forces based on unsaturated soil mechanics, case study: Khangiran, Sarakhs. Amirkabir Journal of Civil Engineering, 2024; 56: 885-908. doi:10.22060/ceej.2024.22616.8006.

[8] Baradaran, S., Aliha, M. R. M. Mode I and Mode II fracture assessment of green asphalt pavements containing plastic waste and RAP at low and intermediate temperature. Results in Engineering, 2025; 25: 103734. doi:10.1016/j.rineng.2024.103734.

[9] Baradaran, S., Ziaee, S. A. Review of the Mechanical Properties of Asphalt Pavement Reinforced with Natural Plant Fibers as an Eco-Friendly Solution in Pavement Engineering. Road, 2025; 33: 167-192. doi:10.22034/road.2025.471341.2308.

[10] Akhtarpour, A., Khodaii, A. Nonlinear Numerical Evaluation of Dynamic Behavior of an Asphaltic Concrete Core Rockfill Dam (A Case Study). Journal of Seismology and Earthquake Engineering, 2009; 11: 143-152.

[11] Niri, S. R., Akhtarpour, A., Daliri, F., Baradaran, M. S. Experimental investigation of dewatering silty tailings using electrokinetic method. Canadian Geotechnical Journal, 2025; 62: 1-25. doi:10.1139/cgj-2024-0069.

[12] Abdulameer AlNaddaf, H. Q., Kouzegaran, S., Fattah, M. Y., Akhtarpour, A. Effects of Cement Treatment on Water Retention Behavior and Collapse Potential of Gypseous Soils: Experimental Investigation and Prediction Models. Advances in Civil Engineering, 2024; 2024: 6637911. doi:10.1155/2024/6637911.

[13] Wang, X., Gao, Y., Jiang, X., Zhang, Q., Liu, W. Analysis on the Characteristics of Water Pollution Caused by Underground Mining and Research Progress of Treatment Technology. Advances in Civil Engineering, 2021; 2021: 9984147. doi:10.1155/2021/9984147.

[14] Mineo, S. Groundwater and soil contamination by LNAPL: State of the art and future challenges. Science of The Total Environment, 2023; 874: 162394. doi:10.1016/j.scitotenv.2023.162394.

[15] Abbas, S. Z., Rafatullah, M. Recent advances in soil microbial fuel cells for soil contaminants remediation. Chemosphere, 2021; 272: 129691. doi:10.1016/j.chemosphere.2021.129691.

[16] Baradaran, M. S., Aftabi Sani, A., abrishami, S. Application of Differential Transform Method for Solving Free-Surface Seepage Problem of One-Dimensional Porous Media. Ferdowsi Civil Engineering, 2024; 37: 1-18. doi:10.22067/jfcei.2024.82170.1226.

[17] Baradaran, M. S., Qazanfari, R., Baradaran, S. Study of soil reinforcement in the east of Mashhad using glass granule. Materials Research Express, 2023; 10: 055202. doi:10.1088/2053-1591/acd5af.

[18] Pargar, J., Akhtarpour, A., Baradaran, M. S. An Unsaturated Soil Mechanics-Based Numerical and Experimental Method to Assess Soil Settlement Due to Ground Water Level Rise. Transportation Infrastructure Geotechnology, 2024; 11: 3621-3646. doi:10.1007/s40515-024-00422-6.

[19] Tareghian, B., Baradaran, M. S., Akhtarpour, A. The effect of sand-crumb rubber mixture treatment on the seismic response of a low-rise building located on liquefiable soil. Discover Geoscience, 2024; 2: 11. doi:10.1007/s44288-024-00014-4.

[20] Pournoori, P., Davarpanah T.Q, A., Rajaee, A., Ghodratnama, M., Abrishami, S., Masoodi, A. R. Experimental exploration of fracture behavior (pure mode III) in eco-friendly steel fiber-reinforced self-compacting concrete with waste tempered glass as coarse aggregates. Scientific Reports, 2024; 14: 9043. doi:10.1038/s41598-024-58912-z.

[21] Eltarabily, M. G. A., Negm, A. M. Numerical Simulation of Fertilizers Movement in Sand and Controlling Transport Process via Vertical Barriers. International Journal of Environmental Science and Development, 2015; 6: 559-565. doi:10.18178/IJESD.

[22] Szymański, K., Janowska, B., Iżewska, A., Sidełko, R., Siebielska, I. Method of evaluating the impact of landfill leachate on groundwater quality. Environmental Monitoring and Assessment, 2018; 190: 415. doi:10.1007/s10661-018-6776-2.

[23] Sharma, A., Ganguly, R., Kumar Gupta, A. Impact Assessment of Leachate Pollution Potential on Groundwater: An Indexing Method. Journal of Environmental Engineering, 2020; 146: 05019007. doi:10.1061/(ASCE)EE.1943-7870.0001647.

[24] Javahershenas, M., Nabizadeh, R., Alimohammadi, M., Mahvi, A. H. The effects of Lahijan landfill leachate on the quality of surface and groundwater resources. International Journal of Environmental Analytical Chemistry, 2022; 102: 558-574. doi:10.1080/03067319.2020.1724984.

[25] Alghamdi, A. G., Aly, A. A., Ibrahim, H. M. Assessing the environmental impacts of municipal solid waste landfill leachate on groundwater and soil contamination in western Saudi Arabia. Arabian Journal of Geosciences, 2021; 14: 350. doi:10.1007/s12517-021-06583-9.

[26] Hussein, M., Yoneda, K., Mohd-Zaki, Z., Amir, A., Othman, N. Heavy metals in leachate, impacted soils and natural soils of different landfills in Malaysia: An alarming threat. Chemosphere, 2021; 267: 128874. doi:10.1016/j.chemosphere.2020.128874.

[27] Nyika, J., Dinka, M., Onyari, E. Effects of landfill leachate on groundwater and its suitability for use. Materials Today: Proceedings, 2022; 57: 958-963. doi:10.1016/j.matpr.2022.03.239.

[28] Alao, J. O. Impacts of open dumpsite leachates on soil and groundwater quality. Groundwater for Sustainable Development, 2023; 20: 100877. doi:10.1016/j.gsd.2022.100877.

[29] Zango, M. U., Kassim, K. A., Sa'ari, R., Rashid, M. F. A., Muhammed, A. S., Ahmad, K., Makinda, J. Use of digital image technique to study leachate penetration in biocemented residual soil. Materials Today: Proceedings, 2022; 48: 734-740. doi:10.1016/j.matpr.2021.02.211.

[30] Vafaei, N., Fakharian, K., Sadrekarimi, A. Sand-sand and sand-steel interface grain-scale behavior under shearing. Transportation Geotechnics, 2021; 30: 100636. doi:10.1016/j.trgeo.2021.100636.

[31] Behdad, A., Moradi, M., Afshari Aghajari, A. The Effect of Soil–Cement Barriers in Containing the LNAPL Contaminants Transport in Unsaturated Soil; A Physical Modeling. Soil and Sediment Contamination: An International Journal, 2022; 31: 692-714. doi:10.1080/15320383.2021.2000364.

[32] Buck, R. P., Rondinini, S., Covington, A. K., Baucke, F. G. K., Brett, C. M. A., Camoes, M. F., Milton, M. J. T., Mussini, T., Naumann, R., Pratt, K. W., Spitzer, P., Wilson, G. S. Measurement of pH. Definition, standards, and procedures (IUPAC Recommendations 2002). 2002; 74: 2169-2200. doi:doi:10.1351/pac200274112169.

[33] Schwab, J. J., Li, Y., Bae, M.-S., Demerjian, K. L., Hou, J., Zhou, X., Jensen, B., Pryor, S. C. A Laboratory Intercomparison of Real-Time Gaseous Ammonia Measurement Methods. Environmental Science & Technology, 2007; 41: 8412-8419. doi:10.1021/es070354r.

[34] Nasrabadi, T., Ruegner, H., Sirdari, Z. Z., Schwientek, M., Grathwohl, P. Using total suspended solids (TSS) and turbidity as proxies for evaluation of metal transport in river water. Applied Geochemistry, 2016; 68: 1-9. doi:10.1016/j.apgeochem.2016.03.003.

[35] Kayaalp, N., Ersahin, M. E., Ozgun, H., Koyuncu, I., Kinaci, C. A new approach for chemical oxygen demand (COD) measurement at high salinity and low organic matter samples. Environmental Science and Pollution Research, 2010; 17: 1547-1552. doi:10.1007/s11356-010-0341-z.

[36] Siwiec, T., Kiedrynska, L., Abramowicz, K., Rewicka, A. L. E. K. S. A. N. D. R. A., Nowak, P. BOD measuring and modelling methods – review. Annals of Warsaw University of Life Sciences, 2011; 43: 143–153. doi:10.2478/v10060-008-0100-8.

[37] Boerlage, S. F. E. Measuring salinity and TDS of seawater and brine for process and environmental monitoring—which one, when? Desalination and Water Treatment, 2012; 42: 222-230. doi:10.5004/dwt.2012.2827.

[38] Alwan, A. H., Al-Adili, A. Numerical Analysis of Water and Crude Oil Flux from Clayey Soil by GeoStudio-SEEP/W. In: Geotechnical Engineering and Sustainable Construction; 2022 March 20; Singapore. p. 191-206. doi:10.1007/978-981-16-6277-5_16.

[39] Harish Kumar Reddy, P., Ramya Krishna, V., Srinivas, K. Design of landfill liners for fine grained soils using CTRAN/W. Materials Today: Proceedings, 2021; 45: 3413-3418. doi:10.1016/j.matpr.2020.12.857.

[40] Lu, N., Likos William, J. Suction Stress Characteristic Curve for Unsaturated Soil. Journal of Geotechnical and Geoenvironmental Engineering, 2006; 132: 131-142. doi:10.1061/(ASCE)1090-0241(2006)132:2(131).

[41] Kuo, J. Practical Design Calculations for Groundwater and Soil Remediation. 2nd ed. Florida (US): CRC Press; 2014. doi:10.1201/b17013.